

# Using city-wide mobile noise assessments to estimate bicycle trip annual exposure to Black Carbon

Luc Dekoninck<sup>a)</sup>  
Dick Botteldooren<sup>b)</sup>  
Information Technology, Acoustics Group, Ghent University  
St-Pietersnieuwstraat 41, 9000 Ghent, Belgium<sup>a,b</sup>

Luc Int Panis<sup>c,d)</sup>  
Flemish Institute for Technological Research (VITO), Boeretang 200, 2400 Mol, Belgium<sup>c</sup>  
Transportation Research Institute (IMOB), Hasselt University, Wetenschapspark 5 bus 6, 3590 Diepenbeek, Belgium<sup>d</sup>

## ABSTRACT

Several studies have shown that a significant amount of daily air pollution exposure, in particular Black Carbon (BC), is inhaled during bicycle trips. Previously, the instantaneous BC exposure of cyclists was modeled as the sum of a background concentration and a local traffic related component based on a local assessment of traffic noise. We present a fast and low cost methodology to achieve a city-wide assessment of yearly average BC exposure of cyclists along their trips, based on a city-wide mobile noise sensing campaign.

The methodology requires participatory sensing measurements of noise, partially combined with BC and/or other air pollutants sensitive to local traffic variations. The combined measurements cover the spatial and meteorological variability and provide the data for an instantaneous exposure model. The mobile noise-only measurements map the full city; and yearly meteorology statistics are used to extrapolate the instantaneous exposure model to a yearly average map of in-traffic air pollution exposure. Less than four passages at each segment along the network with mobile noise equipment are necessary to reach a standard error of 500 ng/m<sup>3</sup> for the yearly average BC exposure.

A strong seasonal effect due to the BC background concentration is detected. The background contributes only 25% to the total trip exposure during spring and summer. During winter the background component increases to 50-60%. Engine related traffic noise along the bicyclist's route is a valid indicator of the BC exposure along the route, independent of the seasonal background. Low exposure route selection results in an exposure reduction of 35% in winter and 60% in summer, sensitive to the weather conditions, specific trip attributes and the available alternatives.

The methodology is relevant for further research into the local effects of air pollution on health. Mobile noise mapping adds local traffic data including traffic dynamics into the air pollution exposure assessments. Local policy makers and urban planners can use the results to support the implementation of low exposure infrastructure, create awareness through route planners and achieve behavioral changes toward active travel modes.

## Highlights

- Mobile noise level to within 2 dB is sufficient to estimate annual BC exposure of cyclists
- Mapping mobile noise provides city-wide yearly averaged in-traffic air pollution exposure
- A low-cost methodology for city-wide evaluation of noise and air pollution is presented
- Cyclists can reduce exposure by 35-60% through selecting low exposure routes

<sup>a)</sup> email: [luc.dekoninck@intec.ugent.be](mailto:luc.dekoninck@intec.ugent.be) (corresponding author, tel +32 9 264 99 95)

<sup>b)</sup> email: [dick.botteldooren@intec.ugent.be](mailto:dick.botteldooren@intec.ugent.be)

<sup>c)</sup> email: [luc.intpanis@vito.be](mailto:luc.intpanis@vito.be); [luc.intpanis@uhasselt.be](mailto:luc.intpanis@uhasselt.be)

45 **Keywords:** Black Carbon, Vehicle Noise, Personal exposure, Cyclists, Traffic, Active mobility

## 46 **1. Introduction**

47 Exposure to particulate matter is currently regulated in PM standards that only distinguish between the  
48 size of the particles but not between the composition and thus origin of the particulate matter. The soot  
49 fraction or Black Carbon (BC) is a fraction of the PM directly related to combustion processes. Recent  
50 evidence, summarized by the World Health Organization (WHO), documents the relevance of BC for  
51 evaluating traffic related health effects (WHO Europe, 2012). BC is more sensitive to traffic emissions and is  
52 able to detect local exposure differences not available in the PM<sub>10</sub> evaluations. The first epidemiological  
53 results based on BC exposure detect health effects up to ten times stronger compared to the similar  
54 evaluations based on PM<sub>10</sub> (Janssen et al. 2011).

55 Large personal exposure measurement campaigns prove the relevance of the in-traffic exposure  
56 contribution to daily personal exposure (Dons et al., 2011, 2012). Technology for mobile air pollution  
57 measurements is however scarce and expensive. The high variability of the in-traffic exposure is partially due  
58 to the strong influence of meteorology on the exposure, swamping the variability due to the local traffic  
59 densities and dynamics (Dons et al., 2013). In previous work of the authors, an instantaneous spatiotemporal  
60 model based on mobile noise measurements for cyclists was proposed (Dekoninck et al., 2013). It was shown  
61 that noise measurements are a good proxy for local traffic intensity and local traffic dynamics. The  
62 instantaneous spatiotemporal model splits the BC exposure of a cyclist into a background component and a  
63 component of local origin. In the Flemish region, only one continuous monitoring station was available at the  
64 time of the measurement campaign that can act as a background concentration (Antwerpen-Linkeroever –  
65 40AL01). After adjusting for the background contribution the local variation in the traffic density and traffic  
66 dynamics successfully predicts the BC exposure of the cyclists using four parameters: the low frequency noise  
67 ( $L_{OLF}$ ) related to the traffic volume and engine throttle, the difference between high and low frequencies  
68 ( $L_{HFmLF}$ ) relating to the traffic speed, the instantaneous wind speed and the street canyon index (StCan). Wind  
69 speed and street canyon features affect the dispersion of BC. The background adjusted model significantly  
70 reduced the temperature dependency of the bicyclist exposure. All temperature dependency, regardless of  
71 the origin (other BC sources, meteorology or vehicle fleet related aspects) is resolved in the background  
72 contribution. In other work, the instantaneous model approach was validated in completely different traffic

73 conditions (Bangalore, India). The quality of the background adjustment was related to the properties of the  
74 background measurement location (Dekoninck et al, 2015). Meteorological conditions thus enter this model  
75 directly through the wind speed and indirectly via temperature and wind speed in the background BC  
76 concentration. Wind direction was not included in the model. The strongest component in the local traffic  
77 related exposure is the traffic within meters from the cyclists, resulting in correlation of 0.86 with only four  
78 parameters. Wind direction is not relevant at such small distances to the source. The noise measurements  
79 quantify the local traffic and traffic dynamics. The strengths of the method are based on the possibility to  
80 quantify the local traffic properties and by adding missing traffic data at low density traffic roads.

81 For many applications however, there is a strong interest in annual average rather than instantaneous  
82 levels of exposure. The internal validation of the instantaneous model -predicting 25% of the trips using  
83 models fit on the other 75% of the trips- resulted on average in a correlation of the trip averaged BC exposure  
84 of 0.77 (Dekoninck et al., 2013). The intrinsic quality of the instantaneous model to predict a single trip under  
85 any meteorological conditions or trajectory is strong and enables the simulation of yearly average exposure  
86 during bicycle trips without further validation. One of the remaining questions is whether subtracting a  
87 measured background concentration results in a valid local contribution that can actually be interpreted as  
88 the contribution of the local traffic ( $BC_{loc}$ ). If this is the case, the model should result in  $BC_{loc}$  approaching zero  
89 with low traffic intensity. As an alternative, the behavior of the strongest component in the spatiotemporal  
90 model,  $L_{OLF}$  is proposed as a good indicator of the background adjustment since this component is directly  
91 related to the presence of traffic. When the spatiotemporal model reveals a linear relationship between  $L_{OLF}$   
92 and  $\log(BC_{loc})$ , the background adjusted exposure will by consequence only include local traffic related  
93 exposure. For low  $L_{OLF}$ , the local contribution in the instantaneous model dwindles to values close to the  
94 detection limit of the BC measurement equipment. Therefore the background location and the applied  
95 background correction are valid.

96 In each mobile measurement campaign only a limited number of potentially occurring situations is  
97 sampled. Bias is introduced into the measurements due to the combination of route choice, instantaneous  
98 meteorological conditions and instantaneous background exposure, each of them subject to unintended  
99 selection bias. It is therefore impossible to perform a measurement campaign covering all combinations of the  
100 exposure variables with unbiased exposure as the result. This paper will therefore introduce a methodology

101 to convert a map of biased mobile measurements into a yearly average unbiased BC exposure map building  
102 upon the available instantaneous model (Dekoninck et al., 2013). This will be achieved in two phases. First  
103 the instantaneous exposure will be extrapolated to a yearly average by applying the spatiotemporal model for  
104 all meteorological situations to all available mobile noise measurements. In the second phase the  
105 instantaneous noise exposure is replaced by the average noise exposure at that location. In this way all  
106 dependence on meteorology can be removed, and the typical traffic situation at each location along the  
107 network is characterized using mobile noise measurements from a small but sufficient number of passages.  
108 This results in a spatial model, only based on local traffic related features (derived from noise) and a street  
109 canyon index (a parameter describing the accumulation of BC in narrow streets).

110 Several research questions will be addressed: how can a mobile noise measurement campaign be used  
111 to predict the annual average BC exposure for cyclists and how many noise measurement trips are necessary  
112 to reliably estimate the local traffic contribution. In addition, the effect of seasonal meteorological changes on  
113 the local traffic related BC exposure and on the total exposure will be illustrated. The potential exposure  
114 reduction by choosing low exposure routes is quantified.

## 115 **2. Methodology and data processing**

### 116 **2.1 Methodology**

117 The instantaneous model is based on 209 rush hour commuting trips by bicycle from the villages to the  
118 west of Ghent (Belgium) into the city center. More than 75 km of distinct roads were sampled at least 3 times.  
119 The BC measurements are performed with the micro-aethalometer AE51 (Aethlabs.com, San Francisco). The  
120 details are available in Dekoninck et al., 2013 and the supplementary data. The instantaneous log-  
121 transformed model will be referred to as  $BC_{loc,temporal}$  in this paper. The subscript 'temporal' is added to avoid  
122 confusion with the spatial yearly average models that will be developed in this work. Thus, to obtain a  
123 meteorology averaged BC exposure of cyclists, only wind speed and background concentration have to be  
124 accounted for. To implement a correction towards yearly representative meteorological conditions, the  
125 meteorological conditions are categorized according to the meteorological dependencies in  $BC_{loc,temporal}$ : wind  
126 speed and background concentration. A joint distribution over these two variables should be used because

127 background BC concentration itself strongly depends on wind speed. The meteorological classes are  
 128 presented in Section 2.2.

129 To obtain a yearly averaged value, the  $BC_{loc,temporal}$  model is applied for a sufficiently large number of  
 130 bicycle commuting trips passing through each evaluation point along the road network for each combined  
 131 meteorological - background concentration class observed during a year. This means that the instantaneous  
 132 wind speed and background concentration of that specific trip are replaced in the model by the wind speed  
 133 and background concentration of the evaluated meteorological class. For each spatial evaluation point, the  
 134 resulting dataset contains a BC estimate for each noise-measuring trip and each meteo/background class,  
 135  $Met_{cl}$ . A weighted average is applied according to the frequency of occurrence during a year of  $Met_{cl}$ , merging  
 136 the results spatially for all trips passing by at a specific location.

137 In mathematical form, the procedure is summarized as follows. The local contribution to the measured BC  
 138 concentration  $BC_{loc,meas,i,j}$  for a location  $i$  and during a trip  $j$ , is written as:

$$139 \quad BC_{loc,meas,i,j} = BC_{tot,meas,i,j} - BC_{bg,j} \quad (1)$$

140 Using the previously derived model, this contribution is approximated using Generalized Additive Models  
 141 (GAM) (Wood, 2006). Several authors in air pollution research have applied this technique successfully  
 142 (Dominici et al., 2002, Pearce et al., 2011, Li et al., 2013). The modeled BC concentration is obtained for each  
 143 location  $i$  during trip  $j$  as:

$$144 \quad BC_{loc,temporal,i,j} = \exp(\text{gam}BC_{loc,temporal}(L_{OLF,i,j}, L_{HFmLF,i,j}, StCan_i, WS_j)) \quad (2a)$$

$$145 \quad BC_{tot,temporal,i,j} = \exp(\text{gam}BC_{loc,temporal}(L_{OLF,i,j}, L_{HFmLF,i,j}, StCan_i, WS_j)) + BC_{bg,j} \quad (2b)$$

146 Note that all spatiotemporal dependence of the GAM model is implicitly included via the model covariates and  
 147 that the background contribution is assumed location independent. Applying the wind speed and BC  
 148 background concentration for all meteorological conditions  $Met_{cl}$  on each trip  $j$ :

$$149 \quad BC_{loc,year,i,j} = \frac{1}{\sum_{Metcl} w_{Metcl}} \sum_{Metcl} w_{Metcl} (\text{gam}BC_{loc,temporal,i,j}) \quad (3)$$

$$150 \quad BC_{tot,year,i,j} = \frac{1}{\sum_{Metcl} w_{Metcl}} \sum_{Metcl} w_{Metcl} (\text{gam}BC_{tot,temporal,i,j}) \quad (4)$$

151 Note that this result still has a weak dependence on trip number, and thus time, via the measured sound  
 152 parameters and via the chosen route at that specific time. By aggregating all measurement trips to a spatial  
 153 point  $p_i$  along the network, the spatial distribution is obtained:

$$154 \quad BC_{loc,year,i} = \frac{1}{n} \sum_j BC_{loc,year,i,j} \quad (5)$$

$$155 \quad BC_{tot,year,i} = \frac{1}{n} \sum_j BC_{tot,year,i,j} \quad (6)$$

156 Where for each spatial point  $p_i$  the collection of trips  $j$  passing point  $p_i$  contribute to the yearly average. In the  
 157 last phase, the instantaneous noise levels are replaced by the average noise levels at each location  $p_i$ . (eq. 7  
 158 and 8). All meteorological variability is included in the input data (eq. 5 and 6) and no instantaneous  
 159 meteorological covariates are necessary in the yearly meteorology based GAM models (eq. 9 and 10):

$$160 \quad L_{OLF,i,map} = \frac{1}{n} \sum_j L_{OLF,i,j} \quad (7)$$

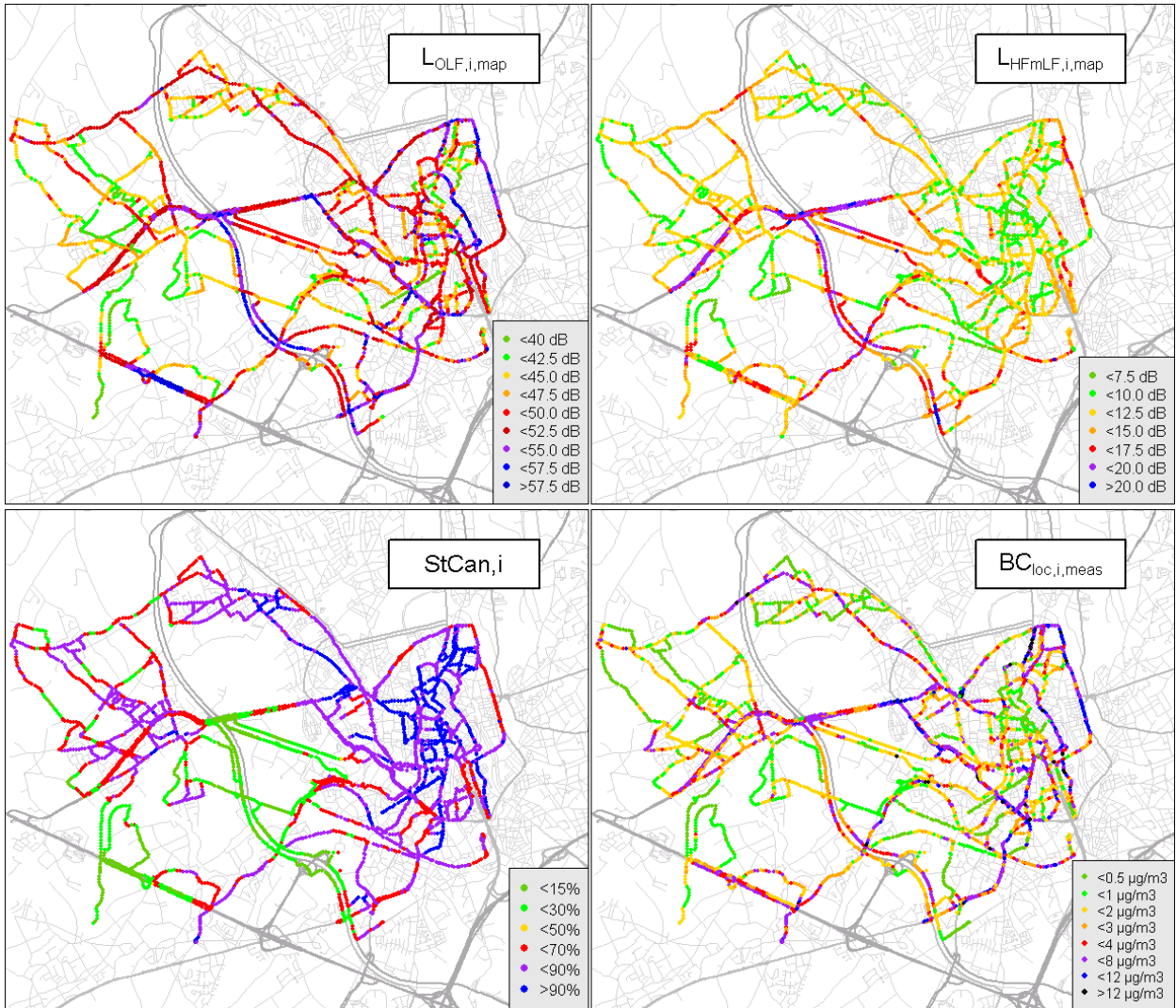
$$161 \quad L_{HFmLF,i,map} = \frac{1}{n} \sum_j L_{HFmLF,i,j} \quad (8)$$

$$162 \quad gamBC_{loc,year} \equiv \log(BC_{loc,year,i}) = gam(L_{OLF,i,map}, L_{HFmLF,i,map}, StCan_i) \quad (9)$$

$$163 \quad gamBC_{tot,year} \equiv \log(BC_{tot,year,i}) = gam(L_{OLF,i,map}, L_{HFmLF,i,map}, StCan_i) \quad (10)$$

164 This results in a function that converts the average mobile noise measurement map to an average BC map,  
 165 independently of the trip sampling paths. In Figure 1, the spatial variability of the two noise covariates  
 166 ( $L_{OLF,i,map}$  and  $L_{HFmLF,i,map}$ ) and the street canyon index  $StCan_i$  are illustrated, as well as the background  
 167 adjusted local component of the BC measurements ( $BC_{loc,meas,i,map}$ ) spatially averaged in a similar way as the  
 168 noise covariates (eq. 7 and 8). Local BC contributions are highly variable and are affected by local traffic  
 169 variability.

170



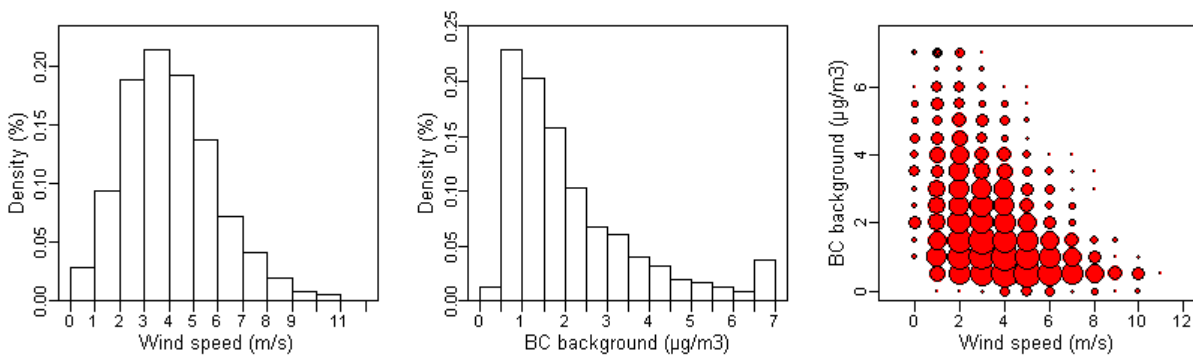
171

172 Figure 1: Three maps showing the spatial covariates ( $L_{OLF,i,map}$ ,  $L_{HFmLF,i,map}$  and  $StCan_i$ ). The fourth map  
173 shows the average local contribution to the BC exposure measurements:  $BC_{loc,i,meas}$ .

## 174 2.2 Meteorology classes

175 The combined mobile noise and BC measurement campaign stretched from November 2010 till  
176 November 2011. The yearly averaged exposure was calculated for the calendar year 2011. A full year of  
177 hourly meteorological data for 2011 was retrieved from the national meteorological institute of Belgium  
178 (KMI). The measuring site is located in Melle, less than 10 km south of the city center of Ghent. BC  
179 background data covering the full year 2011 was made available by the environmental institute of Flanders  
180 (VMM) for the nearest station at Antwerpen-Linkeroever (40AL01). The same data were used for the  
181 background adjustment in the spatiotemporal model. Further information is available at  
182 <http://www.irceline.be>.

183 Only the meteorological conditions during the rush hour (7:00-10:00h and 16:00-19:00h) were included  
 184 in the statistics, since the model is only based on rush hour measurements. For the year 2011 this resulted in  
 185 160 distinct meteorological / background concentration classes (referred to as  $Met_{cl}$ ), each class occurring in  
 186 the year 2011 with a weight  $wMet_{cl,2011}$ . The wind speed classes ranged from 0 to 11 m/s and the BC  
 187 background concentrations from 0 to 16  $\mu\text{g}/\text{m}^3$ . The distribution of the wind speed classes, BC background  
 188 classes and the combined occurrences are presented in Figure 2. The size of the circles is proportional to the  
 189 occurrence  $wMet_{cl,2011}$  of the meteorological situations. The sparse BC background values above 7  $\mu\text{g}/\text{m}^3$  were  
 190 added to the 7  $\mu\text{g}/\text{m}^3$  class for easy presentation in the plot only.



191  
 192 **Figure 2: Histograms of the wind speed (A), BC background exposure (B) and the combined**  
 193 **occurrence of wind speed and background exposure (based on hourly wind speed data in Melle and**  
 194 **30 minute BC data for station 40AL01 obtained respectively from VMM and KMI).**

### 195 3. Results

#### 196 3.1 A model for yearly averaged BC concentration

197 The data processing is based on data from Dekoninck et al, 2013, referred to as BDS. After applying Eq.(3)  
 198 and (4) on BDS the yearly meteorology adjusted BC exposure is available as  $BC_{year,loc,i,j}$  and  $BC_{year,tot,i,j}$  for each  
 199 location  $i$  and each trip  $j$ . The new datasets are representative for the yearly averaged meteorological  
 200 condition, removing the bias due to the not representative sample of meteorology of the trips that passed at  
 201 location  $i$ . A new GAM model containing only three parameters,  $L_{OLF}$ ,  $StCan$  and  $L_{LFmHF}$ , can be extracted from  
 202 the new dataset, since the variability due to the wind speed is removed. The resulting models,  $gamBC_{loc,year}$   
 203 and the  $gamBC_{tot,year}$  are presented in Table 1. The GAM models are almost trivial and virtually perfect, since  
 204 they are based on the output of the  $BC_{loc,temporal}$  GAM model. The only variability left in these GAM models is

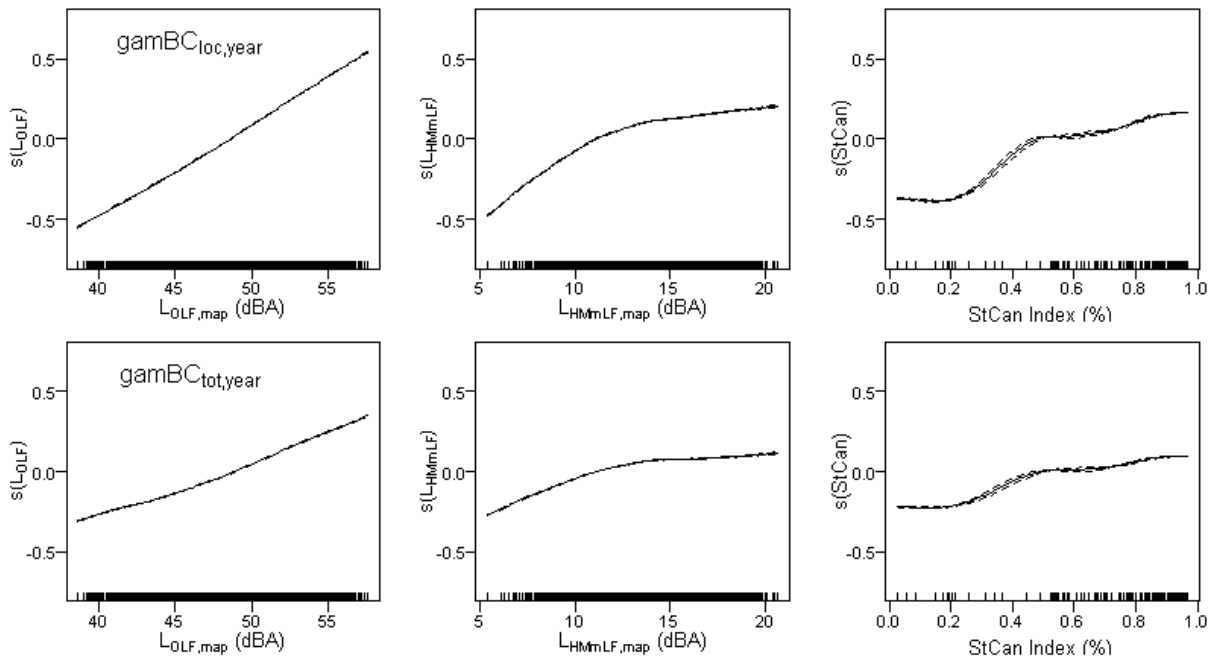


205 the difference in the instantaneous noise evaluation covariates  $L_{OLF}$  and  $L_{HFmLF}$  for the trips contributing to the  
 206 location  $i$ .

Model	Intercept	$L_{OLF,i,map}$	$L_{HFmLF,i,ma}$ $p$	StCan	Deviance explained	Number of points	AIC
		F-value			%	N	
gamBC <sub>loc,year</sub>	8.11 (3.3 $\mu\text{g}/\text{m}^3$ )	37427	10272	18874	99.5	3827	-17064
gamBC <sub>tot,year</sub>	8.60 (5.4 $\mu\text{g}/\text{m}^3$ )	17766	4395	8046	98.9	3827	-17980

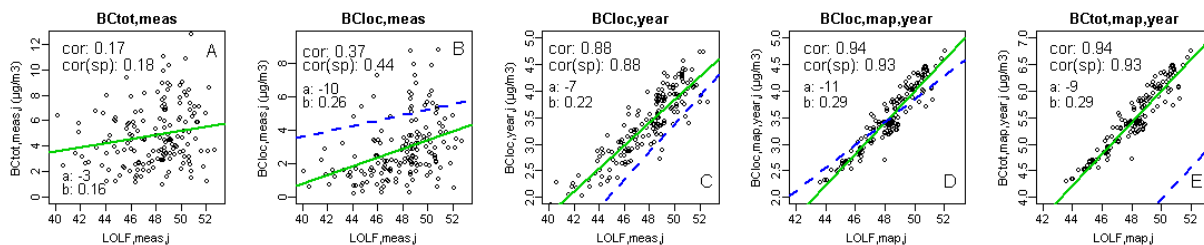
207 **Table 1: Model results comparison, showing intercept, F-values, deviance explained and AIC.**

208 The gamBC<sub>loc,year</sub> model is the strongest model. The engine related noise covariate  $L_{OLF}$  is the strongest  
 209 component in both models. In Figure 3, the three spline plots including the residuals for  $L_{OLF}$ ,  $L_{HFmLF}$  and StCan  
 210 are shown for gamBC<sub>loc,year</sub> and gamBC<sub>tot,year</sub>. In gamBC<sub>tot,year</sub> the low traffic condition (small  $L_{OLF}$ ) converges to  
 211 an lower limit, related to the yearly average BC background concentration. In the  $L_{OLF}$  covariate of  
 212 gamBC<sub>loc,year</sub> a very linear relation is found, even for low values. Traffic evaluation through noise assessment  
 213 has a perfect linear log-log relationship with the engine related noise after adjusting for the yearly  
 214 meteorology distribution. The speed related covariate  $L_{HFmLF}$  converges to a maximum. In situations with high  
 215 traffic speed the BC exposure does not increase any further for equal  $L_{OLF}$ . In the street canyon index a step-  
 216 like solution is visible. Below 0.5 the location is in rather open area, above 0.5, dispersion is significantly  
 217 reduced.



219 **Figure 3: Splines of three covariates of the  $\text{gamBC}_{\text{loc,year}}$  (top) and  $\text{gamBC}_{\text{tot,year}}$  (bottom) models**  
 220 **show strong linear behavior between the OLF and  $\log(\text{BC})$ . In the total exposure the effect of the**  
 221 **background exposure emerges, limiting the decrease of the exposure for low OLF.**

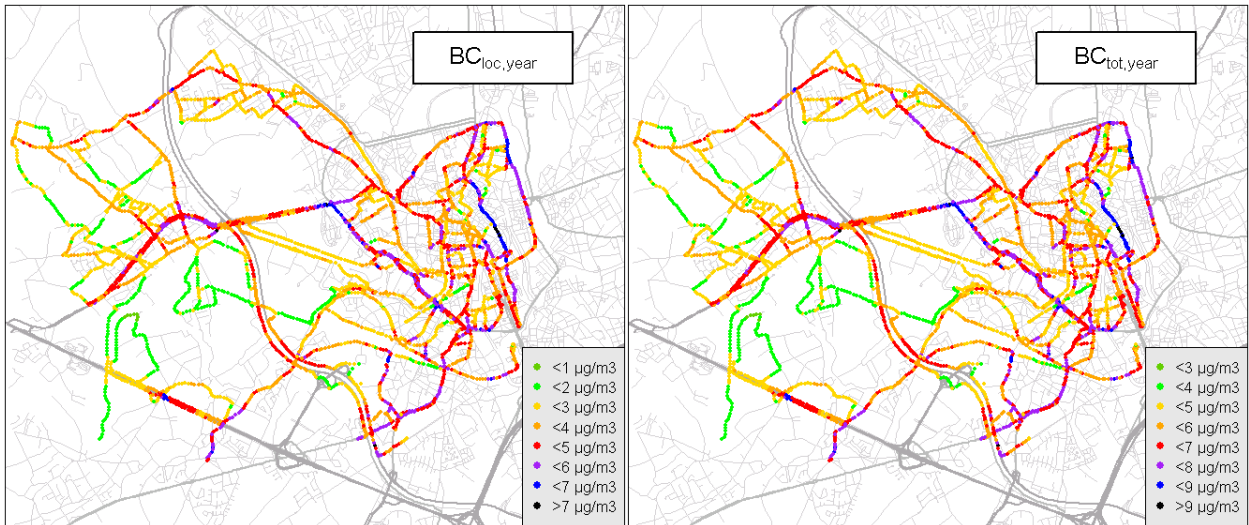
222 Now we illustrate the effect of the different steps in modeling the yearly meteorology adjusted BC  
 223 exposure using mobile noise data. A sequence of evaluations in Figure 4 illustrates the consecutive  
 224 adjustments of the meteorology related effects on the bicyclist's exposure. The first evaluation (plot A) shows  
 225  $\text{BC}_{\text{tot,meas},j}$ , the averaged measured BC exposure by trip (each dot is one trip) as a function of the strongest  
 226 covariate  $L_{\text{OLF,meas},j}$ , the averaged measured noise level  $L_{\text{OLF}}$  along trip  $j$ . The correlation is low. After adjusting  
 227 the exposure for the background contribution ( $\text{BC}_{\text{loc,meas},j}$ ) in plot B the correlation increases, but the wind  
 228 speed is still an important variable in the personal exposure (see Dekoninck et al, 2013). The linear fit of the  
 229 previous plot is repeated in the dashed line as a reference for each of the consecutive steps. In plot C the  
 230 exposure is extrapolated to the yearly average meteorological conditions  $\text{BC}_{\text{loc,year},j}$  for each trip  $j$ . The  
 231 correlation is enhanced up to 0.88 expressing the removal of the meteorology induced bias in the mobile  
 232 measurement campaign. Several of the extremely high exposure trips are drastically reduced by applying the  
 233 yearly average meteorology. The y-axis is adjusted to the new range. Plot D investigates the effect of replacing  
 234 the actual noise measured along the trip by the average noise level for all passages at each location  $i$  passed  
 235 by trip  $j$ , thus evaluating the trips according to the average mobile noise map for both noise covariates  
 236  $L_{\text{OLF},i,\text{map}}$  and  $L_{\text{HFmLF},i,\text{map}}$ . Only a small change is detected for shifting from instantaneous noise level to the  
 237 average over multiple passages, supporting the validity of replacing the instantaneous noise levels by the  
 238 average noise levels. The correlation increases due to the removal of differences in the noise evaluation for  
 239 trips passing at the same location  $i$ . Plot E replaces  $\text{BC}_{\text{loc,year},j}$  by  $\text{BC}_{\text{tot,year},j}$ . The correlation is not affected since  
 240 the difference is only related to the change in background exposure. The yearly average background  
 241 adjustment is added.



242  
 243 **Figure 4: Visual representation of the sequential improvements of mobile measurements as a**  
 244 **function of the trip average engine noise  $L_{\text{OLF}}$ : average measured  $\text{BC}_{\text{tot,meas},j}$  (A) along the trip and**  
 245 **different exposure modeling steps:  $\text{BC}_{\text{loc,meas},j}$ ,  $\text{BC}_{\text{loc,year},j}$ ,  $\text{BC}_{\text{loc,year},\text{map},j}$  and  $\text{BC}_{\text{tot,year},\text{map},j}$  (B, C, D, E). Each**

246 **plot includes a linear fit on the trip evaluation (green). The linear fit of the previous plot is repeated**  
247 **in dashed blue on the next plot. Note the changes in the x and y-axis in the different steps.**

248 The spatial result of the  $\text{gamBC}_{\text{loc,year}}$  and  $\text{gamBC}_{\text{tot,year}}$  is presented in Figure 5. These maps are the yearly  
249 meteorological adjusted version of  $\text{BC}_{\text{loc,meas},i}$  as presented in Figure 1. The maps are much smoother due to  
250 the removal of meteo-related variability. They illustrate the sensitivity of the exposure to the local amount of  
251 traffic, traffic dynamics and the distance of the bicyclist to the local traffic. The difference between  $\text{BC}_{\text{loc,year}}$   
252 and  $\text{BC}_{\text{tot,year}}$  is a constant, the yearly averaged background adjustment.



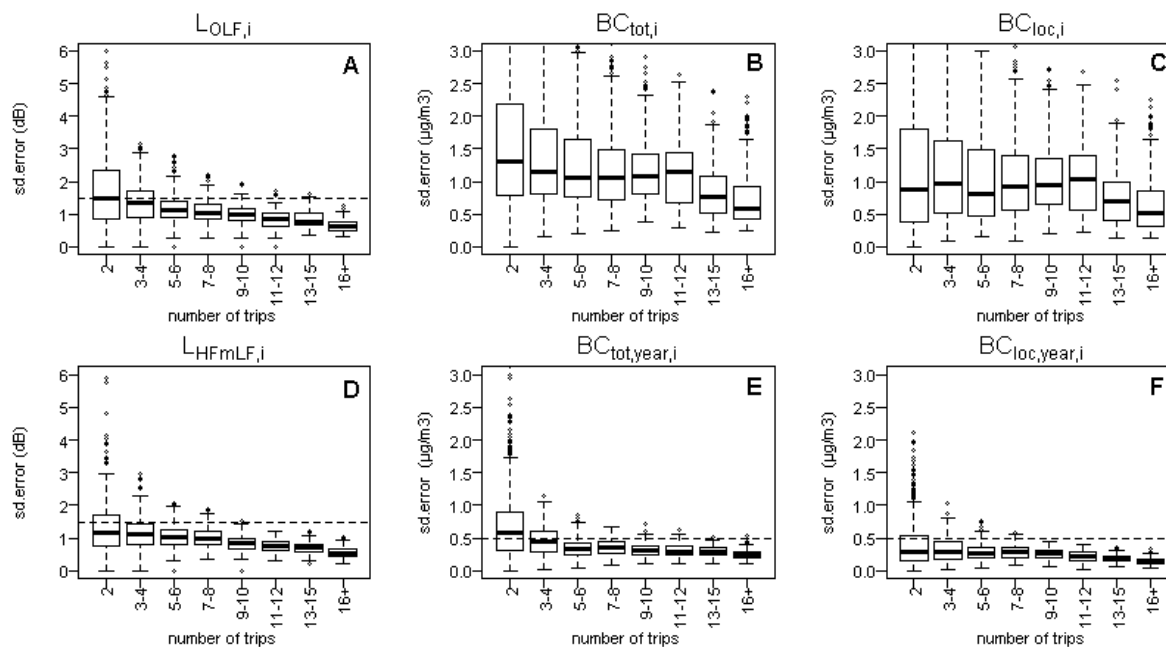
253

254 **Figure 5: Visual representation of the yearly meteorology adjusted and noise mapped exposure**  
255 **based BC exposure for cyclists: local component  $\text{BC}_{\text{loc,year}}$  (left) and total exposure  $\text{BC}_{\text{tot,year}}$  (right).**

### 256 **3.2 Number of noise measurements necessary for yearly** 257 **averaged BC prediction**

258 Since bicyclist's BC exposure is highly sensitive to the meteorology, it is virtually impossible to achieve a  
259 representative sample of measurements for all possible combinations of local traffic and meteorological  
260 situations at a given location. Since the noise exposure at location  $i$  is not sensitive to the BC background  
261 concentrations and much less sensitive to wind speed and wind direction compared to BC exposure, it is  
262 expected that much less measurement repetition will be needed to quantify the local noise exposure at  
263 location  $i$  compared to BC exposure. Hence, the measurement error on the yearly averaged BC exposure is  
264 also expected to drop considerably with increasing number of trips. To confirm this expectation, the  
265 measurement error (standard deviation over all trips divided by the square root of the number of trips that  
266 contribute to the average) is calculated for each location  $i$  with two or more passages. Figure 6 shows box plot

267 statistics over all locations of this standard error for six parameters:  $L_{OLF,i}$ ,  $L_{HFmLF,i}$ ,  $BC_{tot,meas,i}$ ,  $BC_{loc,meas,i}$ ,  
 268  $BC_{tot,year,i}$  and  $BC_{loc,year,i}$  as a function of the number of passages  $n$ . For  $BC_{tot,meas,i}$  the standard error is not  
 269 significantly improving with increasing number of passages if the number of passages is below 10, illustrating  
 270 the high meteorology induced variability. That conclusion is also valid for  $BC_{loc,meas,i}$ , which is surprising since  
 271 a large portion of the meteorological effects is already removed from the dataset by adjusting for  
 272 instantaneous background exposure. For the yearly meteorology adjusted  $BC_{tot,year,i}$  the standard error is  
 273 reduced dramatically. With as little as four passages, the Q3 of the standard error of  $BC_{loc,year,i}$  is smaller than  
 274  $0.5 \mu\text{g}/\text{m}^3$ . In this dataset 95% of all locations have a standard error for  $L_{OLF}$  below 2.0 dB and result in a  
 275 standard error below  $0.5 \mu\text{g}/\text{m}^3$  for  $BC_{loc,year,i}$ . For  $BC_{tot,year,i}$  four passages result in a Q3 smaller than 0.7.  
 276  $\mu\text{g}/\text{m}^3$  and 90% of all locations in this dataset have a standard error for  $L_{OLF}$  below 2.0 dB and result in a  
 277 standard error below  $0.75 \mu\text{g}/\text{m}^3$ . Evaluating  $L_{OLF}$  within 2 dB accuracy is more than sufficient to characterize  
 278 the yearly averaged traffic related BC exposure.

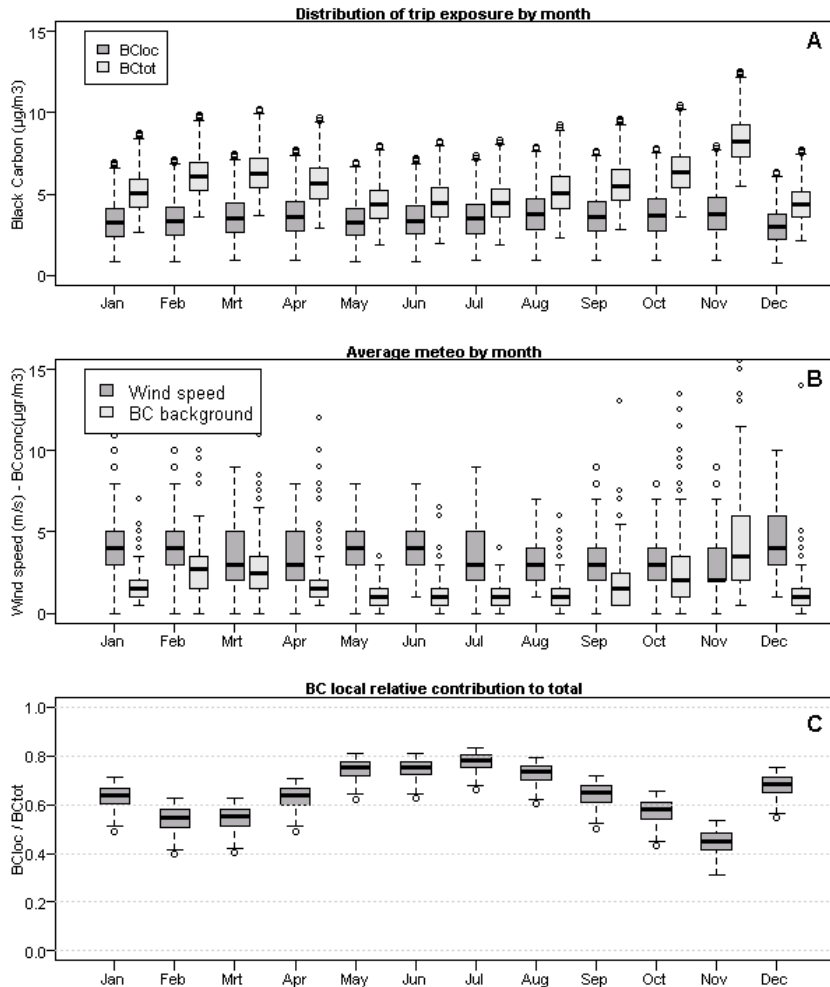


279

280 **Figure 6: Distributions of the standard error by number of passages at location  $i$  for  $L_{OLF,i}$ ,**  
 281  **$BC_{tot,meas,i}$ ,  $BC_{loc,meas,i}$ ,  $L_{HFmLF,i}$ ,  $BC_{tot,year,i}$  and  $BC_{loc,year,i}$ . Drop lines at 1.5 dB and  $0.5 \mu\text{g}/\text{m}^3$  are added for**  
 282 **comparison.**

### 3.3 Monthly variation in BC exposure

283  
284 In many countries the actual use of bicycles and the time spent outdoors depends on weather conditions  
285 and season. Hence, to correctly assess the yearly averaged exposure as well as to give advice to reduce  
286 personal exposure, one may need to account for the annual variation in meteorological conditions. In Figure  
287 7A the evaluation over all trips is presented, while restricting the meteorological weighting to the occurrence  
288 of the meteorological conditions for that specific month:  $BC_{loc,month,j}$  and  $BC_{tot,month,j}$ . The distributions indicate  
289 the range of the high to low exposure trips. The corresponding monthly meteorological statistics for the wind  
290 speed and background concentrations are shown in Figure 7B. Note the atypical conditions in December  
291 2011 with high wind speeds and low background exposure. The variability of the wind speed by month does  
292 not show a strong seasonal pattern, and since this is the only meteorological covariate in the GAM model for  
293  $BC_{loc,month,j}$ ,  $BC_{loc,month,j}$  does not show a seasonal pattern either. In this local situation, a yearly representative  
294 sample of wind speeds occurs each month. A strong seasonal effect on the  $BC_{tot,year,j}$  is visible, expressing the  
295 strong seasonal effect of the background exposure. In Figure 7C the relative contribution of the background  
296 exposure to the local traffic component is shown. In summer, the local contribution is almost 75% of the total  
297 contribution, in winter it drops to 50%. For the larger part of the year, the local contribution is more than  
298 60% of the total exposure.



299

300 **Figure 7: Monthly variation of the distribution of the local and total BC exposure by trip (A).**  
 301 **Background BC and Wind speed show the effect of changing meteorological conditions over the year**  
 302 **(B). Relative contribution of the local contribution to the total exposure (C).**

### 303 3.4 City-wide mapping and low exposure routes

304 The proposed methodology for data collection uses mobile measurements on bicycle and consists of two  
 305 simultaneous actions: during a limited set of trips BC and noise are measured jointly, preferably covering the  
 306 full range of meteorological conditions and traffic conditions. These data are used to tune the coefficients in a  
 307 local version of the  $BC_{loc,temporal}$  model to the specific emission of the local vehicle fleet, meteorological  
 308 conditions and background concentrations. The  $BC_{loc,temporal}$  model is converted to the yearly meteorology  
 309 adjusted GAM models as described in 2.1. An extensive mobile noise only measurement campaign can be  
 310 performed to obtain spatial detail for a more extended area. In a numerical example: a city-wide participatory  
 311 campaign with ten cheap noise measurement units, used by one-hundred participants for two weeks each can  
 312 be completed in half a year. With a typical bicycle route of 10 km, each measuring their standard route and a

313 set of alternatives, will result in approximately 100 persons x 20 trips x 10 km or 20,000 km of mobile noise  
314 data. If the participants' origins and destinations are well distributed over the investigated city and suburbs,  
315 the majority of roads will be sampled adequately. The mobile noise measurements result in city-wide noise  
316 maps  $L_{OLF,i,map}$  and  $L_{HFmLF,i,map}$ . Mapping any bicycle trajectory to the mobile noise maps (within the extent of  
317 the map) and applying the  $BC_{loc,temporal}$  results in an instantaneous meteorological sensitive estimate of the BC  
318 trip exposure. Applying the yearly or monthly meteorology adjusted models results in yearly or monthly  
319 averaged BC exposure, according to the requirements of the application.

320 To estimate the potential exposure improvement of alternative route choice, we take a closer look at the  
321 trips used for deriving the models presented in this article (Figure 4). Figures 4D and 4E show that trips  
322 performed during rush hour result in differences in  $L_{OLF}$  of up to 10 dB with a matching reduction of over  
323 50% in  $BC_{loc,year}$  and 35% in  $BC_{tot,year}$ . A reference trip with an average  $L_{OLF,map,trip}$  of 50 dB and an alternative  
324 trip of 46 dB will result in a decrease of 1.3  $\mu\text{g}/\text{m}^3$ , a reduction of 33% for the local traffic component and  
325 22% on the total exposure in a far from extreme trip change scenario. In interpreting the results one should  
326 take into account that the travelled routes in this dataset were not optimized to detect the low exposure  
327 routes. The travelled routes were by design always switching from high to low exposure road segments to  
328 capture as much variability in traffic for similar meteorological conditions within a single trip. A systematic  
329 choice for a low exposure route for commuting could easily result in a 35 to 60% reduction in personal  
330 exposure depending on the season, but this also depends on the specific commute and the available  
331 alternatives for that trip.

## 332 4. DISCUSSION

### 333 4.1 Predictive quality of the methodology

334 At first sight the GAM models deviance explained is extremely high. When considering the procedure and  
335 the importance of the wind speed covariate in the spatiotemporal model, this is not surprising. All remaining  
336 variability that is not explained by the spatiotemporal model is -by design- not available in the yearly  
337 extrapolation. More important than the fact that the  $gamBC_{loc,year}$  and  $gamBC_{tot,year}$  models are virtually  
338 perfect, is that all locations are included, even those that were sampled only once or twice, without affecting  
339 the quality of the GAM model. It was expected that the dataset should be restricted to a minimum number of

340 passages to build a valid GAM model, but this was clearly not necessary. The quality of the model in the  
341 locations with low sampling is also visible in Figures 6E and 6F. 75% of the points with only two passages  
342 reach a yearly standard error below 500 ngr/m<sup>3</sup> for the  $gamBC_{loc,year}$  and almost 50% reach this value for the  
343  $gamBC_{tot,year}$  model. The procedure to adjust each individual trip to the yearly averaged meteorological  
344 situation is effective. Dekoninck et al. (2012) concluded that an estimate of  $L_{OLF}$  resulted in a standard error of  
345 approximately 1.5 dB after ten samples at a specific location in similar traffic conditions. The results in this  
346 paper show that a standard error of 1.5 dB does not have to be achieved to successfully apply this  
347 methodology. A standard error of 2.0 dB is more than sufficient to result in a valid prediction of the yearly BC  
348 exposure, which is achieved with four passages for a specific traffic condition. The data showed that it is  
349 extremely difficult to achieve a valid averaged BC exposure by increasing the number of passages without  
350 using the proposed modeling approach, as illustrated by the low reduction by number of trips in Figures 6B  
351 and 6C. Noise measurements adequately quantify the local traffic situation and enable the disaggregation of  
352 the variability in the BC measurements into local traffic related and meteorology related contributions. This is  
353 valid for the instantaneous model and the yearly meteorology extrapolated model.

## 354 **4.2 Comparison with other mobile measurements**

355 A general review by Bigazzi and Figliozzi (2014) summarized 42 studies on the exposure of bicyclists.  
356 Fourteen studies addressed BC or EC. The studies are combined and evaluated according to the reported  
357 differences between high and low exposure road segments. The exposure on high exposure segments is 8  
358 times higher than low exposure segments across the studies when excluding rural assessments. In the  
359 measurements for the instantaneous model (reported in  $BC_{loc,i,meas}$ ) the high exposure locations reach levels  
360 up to 25 times the low exposure locations when including rural data and up to 10 times when excluding rural  
361 data (see Figure 5). The evaluations in the instantaneous model are aggregated by 50 m segments. In the  
362 review the data is aggregated by physical street segments. The measurements in the instantaneous model  
363 also include high wind speed conditions and extreme background conditions, typically not sampled in bicycle  
364 campaigns. These differences in the measurement setup (spatial detail and sampled meteorological  
365 conditions) explain the larger detected ranges. Despite the differences in the measurement setup, the  
366 measurement ranges are comparable with the results in the review.



### 4.3 Potential of background adjusted models

The additive modeling approach has the potential to be more than a mathematical method to disentangle the meteorological and background exposure effects from the local traffic contribution. Several authors investigated the particle size distribution in relation to the distance to the source (Karner et al., 2010, Boogaard et al., 2011, Strak et al., 2011, Kingham et al., 2013, Holder et al., 2014). All results show similar trends; closer to the source the size distributions show higher numbers of small particles. In health effects of air pollution exposure research, the importance of the particle size and particle count has been investigated by different authors (Strak et al., 2010, Seaton et al., 1995). Although the smallest particles may enter the body in different ways (e.g. through the olfactory nerve (Oberdorster, 2004)), specific health effects or different toxicity estimates (based on particle mass or on particle number and size distributions) have proven hard to detect (Osunsanya et al., 2001). The additive approach -splitting exposure in background particles (aged and larger) and local contribution (fresh and small)- can be a base for adjusting the exposure to particle size corrected exposures and to verify if high local contributions result in adverse health effects. Quantifying the particle size distribution adjustments for the local and background contribution is subject to further research. Similar measurement campaigns measuring UFP particle counts or particle size distributions can add significant value in this respect. A smaller measurement campaign has already shown that this technique is also valid for UFP (Dekoninck et al., 2015). UFP shows a steeper relation to  $L_{OLF}$  compared to BC and the additive approach is less sensitive to the background concentrations compared to BC.

### 4.4 Diurnal variability, vehicle fleet composition and policy support

The main limitation in the presented results is the restriction to rush hour exposure and traffic, the data limitation of the underlying instantaneous model. Since most policy measures are mainly focusing on commuting, the presented results are applicable in that context. The proven effectiveness of the noise sampling implies that mapping the traffic related exposure has the potential to be extended to capture the diurnal variability with only a small extension of the sampling strategy to include trips outside the rush hour and adding the hour of the day as a new dimension in the models. Only few passages on different types of routes for different times of the day could reveal the diurnal patterns of the BC exposure. Implementing this technique in other countries and/or continents requires recalibration of the instantaneous model. Vehicle fleet, vehicle fleet evolution, driver behavior, biking facilities, city characteristics, meteorological conditions

395 and air pollution background concentration all have their specific influence on the relationship between noise  
396 and local traffic related air pollution. The sensitivity of the spatiotemporal model at different locations should  
397 be evaluated for other dependencies (temperature, humidity etc.). Validating new implementations is crucial  
398 and will not only illustrate the proposed methodology but will also detect effects of different vehicle fleets.  
399 This must be seen as one of the most important applications of the combined methods (instantaneous  
400 modeling and yearly meteorology adjusted maps). The instantaneous models will adjust and resolve the bias  
401 between the different mobile measurement campaigns for meteorology, background concentrations, route  
402 choice and traffic dynamics. The remaining difference can be attributed to the different fleet composition. In  
403 Belgium more than 60% of the vehicles use diesel, a well-known source of BC. Large changes in the  
404 relationship between noise and BC in other countries are probable and will be relevant for policy decisions in  
405 Belgium. Consecutive calibration measurement campaigns are relevant to quantify the changes in the vehicle  
406 fleet emission over time and require similar control over the sampling biases to reveal the vehicle fleet  
407 related component in the evolution of the BC exposure. The effects of changes in the local and the background  
408 exposure due to changes in the vehicle fleet emission or other BC sources are automatically included through  
409 the background adjusted approach of the instantaneous model. This leads us to an important feature of the  
410 mobile noise based traffic assessments. Noise emission of the vehicle fleet is much less sensitive to change  
411 over time due to much less restrictive and less effective legislation for the noise emission of the vehicle fleet.  
412 The traffic quantification is therefore valid for longer periods of time. Only reduced combined noise-BC  
413 measurement campaigns are required to reassess the noise-BC relation. In response to local policy based  
414 traffic changes, small dedicated 'noise-only' measurements can reassess the traffic densities and traffic  
415 dynamics. The burden and costs of performing large air pollution measurement campaigns can be reduced  
416 significantly while the results cover much larger areas.

417 From a scientific point of view, the improvement of personal exposure assessment for bicyclists to traffic  
418 related air pollution is the most important goal of this methodological exercise. From the cyclist's point of  
419 view, the awareness of their route choice on the related exposure is the most important aspect. Only if people  
420 are aware of an issue, they can react and change their behavior accordingly. The main traffic related challenge  
421 of the local governments is reducing car use within cities and promoting a shift to other modes of  
422 transportation. A campaign similar to the proposed setup can inform the public on low exposure routes for

423 cyclists and the local government can use this information to improve the quality, availability and  
424 dissemination of the alternative routes. Missing links in the biking network can be detected and benefits of  
425 investing in these trajectories can be quantified and used in the dissemination process. Alternative routes and  
426 improved bicycle infrastructure will also reduce the number of bicycle accidents (Reynolds et al., 2009,  
427 Vandenbulcke et al., 2014, Molino et al., 2009).

## 428 **4.5 Multidisciplinary aspects and LURs**

429 The mobile noise mapping should not be only performed for air pollution assessments but can also be a  
430 part of extended multidisciplinary evaluations of in-city traffic related livability. Strong synergies exist  
431 between local air pollution exposure assessments and traffic noise related burdens. Local traffic assessment  
432 along the roads near the dwellings improves noise annoyance and wellbeing evaluations of the inhabitants  
433 (Botteldooren et al., 2010). Mobile noise measurements include more detail than calculated noise maps and  
434 have the potential to add value to all environmental noise related evaluations. They also provide a proxy for  
435 traffic on low-density roads where no external traffic data is available. An important application is the  
436 improvement of the traffic related air pollution land-use regression models. The mobile noise map provides  
437 traffic data for the LUR models on low density roads including local traffic dynamics. In the acoustic field, the  
438 combination of mobile and fixed noise monitoring stations will enable dynamic noise maps (Can et al., 2011,  
439 Can et al., 2014). City-wide mobile noise evaluation is therefore a strong tool to improve in-city livability in a  
440 multidisciplinary approach.

## 441 **5. CONCLUSIONS**

442 We have successfully extended an instantaneous exposure model for bicyclists to a yearly meteorology  
443 averaged exposure model. Strong seasonal effects were detected. Mapping the local variability of in-traffic  
444 exposure to BC for cyclists based on mobile noise measurements can be achieved with a small number of  
445 passages, since the noise exposure assessments are much less influenced by meteorological conditions and  
446 are therefore more efficient compared to in-traffic air pollution assessments. Extending the presented models  
447 to diurnal exposure models becomes feasible.

448 In low background conditions the background BC exposure accounts for less than 25% of the bicyclist's  
449 exposure, whereas in high background exposure conditions the contribution is 40 to 60%. Low exposure

450 route choice can reduce the local traffic exposure with at least 35-60% depending on the available alternative  
451 trajectories and the season. Local governments can use mobile noise mapping to support investments in  
452 alternative networks for cyclists.

453 The results support the potential of the additive approach defining personal exposure as the sum of a  
454 background contribution and a local traffic contribution. Applying this technique enables international  
455 comparison of both the local traffic related particulate matter exposure and the background exposure levels.  
456 Applying the methodology on a city-wide scale will result in a detailed spatial and accurate yearly averaged  
457 exposure map. The influence of instantaneous meteorology on air pollution exposure can be quantified  
458 through a partial participatory sensing campaign measuring one or more traffic related air pollutants for the  
459 full range of meteorological conditions in parallel to the mobile noise measurement campaign mapping the  
460 full city. Extrapolation to yearly local and total exposure with or without seasonal adjustments is inherently  
461 available in the methodology. This low cost methodology quantifies the local traffic in an unprecedented  
462 spatial resolution and fits in a multidisciplinary approach of evaluating and improving personal exposure,  
463 livability, wellbeing and health in large urban and suburban context.

## 464 **6. REFERENCES**

- 465 Bigazzi, A. Y., & Figliozzi, M. A. (2014). Review of Urban Bicyclists' Intake and Uptake of Traffic-Related Air  
466 Pollution. *Transport Reviews*, 34(2), 221-245.
- 467 Boogaard H., Kos G.P.A., Weijers E.P., Janssen N.A.H., Fischer P.H., et al. 2011. Contrast in air pollution  
468 components between major streets and background locations: Particulate matter mass, black carbon,  
469 elemental composition, nitrogen oxide and ultrafine particle number. *Atmospheric Environment*, 45,  
470 650-658.
- 471 Botteldooren D., Dekoninck L. & Gillis D. 2011. The Influence of Traffic Noise on Appreciation of the Living  
472 Quality of a Neighborhood. *International Journal of Environmental Research and Public Health*, 8, 777-  
473 798.
- 474 Can A., Dekoninck L. & Botteldooren D. 2014. Measurement network for urban noise assessment: Comparison  
475 of mobile measurements and spatial interpolation approaches. *Applied Acoustics*, 83, 32-39.
- 476 Can A., Van Renterghem T., Rademaker M., Dauwe S., Thomas P., et al. 2011. Sampling approaches to predict  
477 urban street noise levels using fixed and temporary microphones. *Journal of Environmental Monitoring*,  
478 13, 2710-2719.

479 Dekoninck, L.; Botteldooren, D.; Int Panis, L., Guidelines for participatory noise sensing based on analysis of  
480 high quality mobile noise measurements. *Internoise 2012 (conference)*, 394-402

481 Dekoninck L., Botteldooren D. & Int Panis L. 2013. An instantaneous spatiotemporal model to predict a  
482 bicyclist's Black Carbon exposure based on mobile noise measurements. *Atmospheric Environment*, 79,  
483 623-631.

484 Dekoninck L., Botteldooren D., Panis L.I., Hankey S., Jain G., et al. 2015. Applicability of a noise-based model to  
485 estimate in-traffic exposure to black carbon and particle number concentrations in different cultures.  
486 *Environment International*, 74, 89-98.

487 Dominici F., McDermott A., Zeger S.L. & Samet J.M. 2002. On the use of generalized additive models in time-  
488 series studies of air pollution and health. *American Journal of Epidemiology*, 156, 193-203.

489 Dons E., Panis L.I., Van Poppel M., Theunis J. & Wets G. 2012. Personal exposure to Black Carbon in transport  
490 microenvironments. *Atmospheric Environment*, 55.

491 Holder A.L., Hagler G.S.W., Yelverton T.L.B. & Hays M.D. 2014. On-road black carbon instrument  
492 intercomparison and aerosol characteristics by driving environment. *Atmospheric Environment*, 88,  
493 183-191.

494 Janssen N.A.H., Hoek G., Simic-Lawson M., Fischer P., van Bree L., et al. 2011. Black Carbon as an Additional  
495 Indicator of the Adverse Health Effects of Airborne Particles Compared with PM<sub>10</sub> and PM<sub>2.5</sub>.  
496 *Environmental Health Perspectives*, 119, 1691-1699.

497 Karner A.A., Eisinger D.S. & Niemeier D.A. 2010. Near-Roadway Air Quality: Synthesizing the Findings from  
498 Real-World Data. *Environmental Science & Technology*, 44, 5334-5344.

499 Li L.F., Wu J., Hudda N., Sioutas C., Fruin S.A., et al. 2013. Modeling the Concentrations of On-Road Air  
500 Pollutants in Southern California. *Environmental Science & Technology*, 47, 9291-9299.

501 Molino J.A., Kennedy J.F., Johnson P.L., Beuse P.A., Emo A.K., et al. 2009. Pedestrian and Bicyclist Exposure to  
502 Risk Methodology for Estimation in an Urban Environment. *Transportation Research Record*, 145-153.

503 Oberdorster G., Sharp Z., Atudorei V., Elder A., Gelein R., et al. 2004. Translocation of inhaled ultrafine  
504 particles to the brain. *Inhalation Toxicology*, 16, 437-445.

505 Osunsanya T., Prescott G. & Seaton A. 2001. Acute respiratory effects of particles: mass or number?  
506 *Occupational and Environmental Medicine*, 58, 154-159.

507 Pearce J.L., Beringer J., Nicholls N., Hyndman R.J. & Tapper N.J. 2011. Quantifying the influence of local  
508 meteorology on air quality using generalized additive models. *Atmospheric Environment*, 45, 1328-  
509 1336.

510 Reynolds C.C.O., Harris M.A., Teschke K., Cripton P.A. & Winters M. 2009. The impact of transportation  
511 infrastructure on bicycling injuries and crashes: a review of the literature. *Environmental Health*, 8.

512 Seaton A., Macnee W., Donaldson K. & Godden D. 1995. PARTICULATE AIR-POLLUTION AND ACUTE HEALTH-  
513 EFFECTS. *Lancet*, 345, 176-178.

514 Strak M., Boogaard H., Meliefste K., Oldenwening M., Zuurbier M., et al. 2010. Respiratory health effects of  
515 ultrafine and fine particle exposure in cyclists. *Occupational and Environmental Medicine*, 67, 118-124.

516 Strak M., Steenhof M., Godri K.J., Gosens I., Mudway I.S., et al. 2011. Variation in characteristics of ambient  
517 particulate matter at eight locations in the Netherlands - The RAPTES project. Atmospheric  
518 Environment, 45, 4442-4453.

519 Vandebulcke G., Thomas I. & Panis L.I. 2014. Predicting cycling accident risk in Brussels: A spatial case-  
520 control approach. Accident Analysis and Prevention, 62, 341-357.

521 WHO Europe, 2012: Health effects of black carbon, ISBN: 978 92 890 0265 3.

522 Wood S.N. 2006. On confidence intervals for generalized additive models based on penalized regression  
523 splines. Australian & New Zealand Journal of Statistics, 48.

524